001

Date: April 17, 1964
Project No. 303200
Copy No. 22

STUDY OF THIN FILM LARGE AREA PHOTOVOLTAIC SOLAR ENERGY CONVERTER

Second Quarterly Report
January 1, 1964 - March 31, 1964
Contract No. NAS3-2795

National Aeronautics and Space Administration
Lewis Research Center
Space Power Systems Division

By: Warren J. Deshotels
Frank Augustine
John Koenig

Approved: Hans Jaffe
Hans Jaffe, Director
Electronic Research

Clevite Corporation
Electronic Research Division
Cleveland, Ohio 44108
216 - 851-5500

NASA CR 54065
Project No. 303200

Second Quarterly Report

STUDY OF THIN FILM LARGE AREA PHOTOVOLTAIC SOLAR ENERGY CONVERTER

by

W.J. Deshotels, F. Augustine, and J. Koenig

Prepared for

NATIONAL AERONAUTICS AND SPACE ADMINISTRATION

April 17, 1964

CONTRACT NAS 3-2795

Technical Management
NASA Lewis Research Center
Cleveland, Ohio
Space Power Systems Division
Mr. C.K. Swartz, MS86-1

Clevite Corporation
Electronic Research Division
Cleveland, Ohio 44108

TABLE OF CONTENTS

LIST OF ILLUSTRATIONS

STUDY OF THIN FILM LARGE AREA PHOTOVOLTAIC SOLAR ENERGY CONVERTER

by

Warren J. Deshotels, Frank Augustine and John Koenig
Electronic Research Division, Clevite Corporation

SUMMARY

This report covers the work performed during the period January 1, 1964 through March 31, 1964, under Contract No. NAS 3-2795 sponsored by the Lewis Research Center, National Aeronautics and Space Administration.

During this period, thirty-three evaporations were completed yielding 301 individual cadmium sulfide films on glass and H-Film substrates. Modifications introduced in the evaporator include: a thermocouple well in the crucible in order to monitor the evaporation temperature; and the installation of new and effective heat shields around the crucible and the substrate heater resulting in a 50 percent reduction in power requirements.

The use of embossed H-Film substrates has significantly reduced the curling of the CdS photovoltaic cells. It is expected that further experimentation with the embossed substrates will essentially eliminate the curling problem. Arrays of nine, 1 $in.^2$, CdS cells have been made on two H-Film substrates, each substrate measuring 4 inches x 4 inches. The individual efficiencies of these cells ranged from 1.3 to 2.6 percent and averaged 2.0 percent for the 18 cells.

A careful examination of vacuum evaporated and electroplated metal contacts to n-type CdS was undertaken. Nickel, chromium and gold were found to make low resistance, ohmic contacts to CdS. While nickel had the lowest contact resistance, gold was judged to be the most convenient, because of its solderability.

A survey of photovoltaic cells, obtained from 149 evaporations, indicated a set of optimum film properties which will be used as a guide in future evaporations.

The deterioration of CdS photovoltaic film cells was studied intensively during this quarter and significant improvements achieved. Several cells, fabricated according to a modification of the standard barrier formation process, exhibited little or no decrease in efficiency as long as 46 days after formation.

Mathematical models are discussed with reference to a unique determination of the rectification quality of CdS photovoltaic cells as expressed by the exponential term in the simple diode equation. The simple model is used to demonstrate the correspondence between cell efficiency and reverse saturation current.

1. INTRODUCTION

Present day operational photovoltaic solar energy converters are made of arrays of small silicon cells. Each array may contain hundreds of individual cells connected in series — parallel to provide the required level of power. Because silicon is subject to radiation damage, the arrays must be shielded by thin sheets of fused silica. Attempts to reduce the number of individual cells by employing large area silicon cells have so far been unsuccessful although recent advances in growing dendritic, thin, silicon films are promising.

Interest in thin film, large area, cadmium sulfide photovoltaic solar energy converters stems from the fact that such cells have been fabricated with areas as large as thirty-six square inches and conversion efficiencies approaching 3 percent. Furthermore, these films can be put on flexible substrates and are presumed to be highly resistant to radiation damage since they do not depend on high crystalline perfection.

The work described herein is based on the backwall cell arrangement in which sunlight is incident on a highly conducting transparent cadmium sulfide layer and is absorbed in an opaque modified cadmium sulfide layer below the transparent layer. Compared to the frontwall cell, under study elsewhere, the backwall cell has two principal advantages: 1) The high conductance of the top, transparent, CdS layer minimizes the area of metal grids or bus bars that have to be placed in the path of the incident radiation. 2) The light sensitive layer is protected from the ambient by the relatively thick transparent CdS layer on one side and may be protected by metal foil or another impervious coating on the other.

The principal purpose of this study is the development of a CdS photovoltaic solar energy converter consisting of a large area transparent plastic substrate on which is an array of closely spaced, small (nominally one-inch square), backwall, CdS photocells connected in series or in parallel, depending upon the desired voltage-current output.

2. EVAPORATED FILM CELLS

Thirty-three evaporations (Nos. 117 through 149) were completed during this quarter. These yielded 180 films on 1 inch x 2 inch glass substrates, 48 films on 1/2 inch x 2 inch glass substrates, eight 3 x 3 arrays of one square inch cells on 4 inch x 4 inch H-Film substrates and one single 4 inch x 4 inch film on an H-Film substrate, making a total of 301 individual films.

2.1 Evaporator

The quartz crucibles with thermocouple well have been used throughout this quarter. The tungsten heater coils proved less satisfactory than the tantalum coils and their use has been discontinued. The tantalum coils require frequent replacement because of their tendency to sag during use. It is expected that a suitably grooved quartz cylinder will be effective in supporting the tantalum coil. One such cylinder was fabricated but the grooves were so deep that the heater coil could not be inserted properly. Another cylinder is being made and will have shallow grooves.

A heat shield has been placed around the crucible. This consists of a double wall quartz cylinder with an insulating material (Fiberfrax) contained between the walls. The amount of power wasted has been greatly reduced resulting in much lower bell jar temperatures.

An aluminum shield has been added to the substrate heater, reducing the time required to bring the substrate up to the desired temperature. These modifications required redetermination of some of the evaporation parameters.

A 3.2 KVA transformer has been obtained to augment the power supplies for the heater coils and substrate heater of the 18 inch vacuum evaporator.

A transistor washer has been obtained and is used for rinsing the substrates before evaporation and for washing the excess slurry from cells during processing.

The addition of the heat shield has altered the time-temperature profile of the crucible. Instead of observing a drop in temperature when the thermocouple in the crucible is uncovered by the evaporating charge, a sharp rise is now observed. The temperature change at this point is still, however, an adequate indication of the evaporation end-point.

All of the modifications described above have been incorporated into the large vacuum system as well as the small one.

Close control of the evaporation parameters permits reproducible evaporations resulting in films meeting a set of specifications for "good" cells. These specifications have been culled from data from more than 140 evaporations and are given in a later section.

2.2 Substrates

Adherence of evaporated CdS to glass and H-Film substrates is significantly improved by roughing the substrate surface. This has been accomplished by lapping or sandblasting. The principal difficulty encountered with both roughing procedures has been inclusion of some of the abrading particles in the surface. These are removed only with laborious cleaning methods. Etching techniques are being investigated. Some sort of fluoride etch will be used on glass substrates while ammonium hydroxide mixtures will be used on H-Film.

The experiments with embossed H-Film have been very encouraging. The die is an array of close packed hemispheres about 0.125 inch diameter. The H-Film is pressed cold onto the die by a rubber platen. CdS films evaporated on embossed H-Film exhibit very little curling and with suitable adjustment of boss diameter and film thickness, it should be possible to eliminate the curling entirely. Several problems still have to be solved. The H-Film tends to tear or split when pressed against the die. This will require some experimentation with embossing pressure, boss diameter and lubrication. Sandblasting the embossed H-Film uniformly is difficult because the resilience of the material inhibits the abrading of the raised portions of the film. The result is good adherence of CdS in the concave portion of the film but poor adhesion to the ridges between hemispheres. A back-up die for sandblasting would take care of this difficulty. A suitable chemical etch would eliminate this problem entirely. Relatively little work has been done on the embossing

problems this quarter. More attention will be devoted to this in the next quarter.

3. PROCESSING OF FILMS

Much of the time this quarter was devoted to a study of photovoltaic cell deterioration. Because of its importance, this work is described in a separate section.

A number of cells on glass substrates were processed in the usual manner and efficiencies as high as 2.2 percent were obtained. This represents a small decrease in highest efficiencies and is attributed to the temporary variations in film quality due to small changes in evaporation parameters accompanying the evaporator modifications described in Section 2.

3.1 CdS Arrays on H-Film

Two CdS arrays on H-Film substrates are worthy of specific mention. Each array consisted of 9 CdS cells, nominally one-inch square, on a 4 inch x 4 inch H-Film substrate. The conversion efficiency of each cell was independently determined:

Array 107H:	1.7	2.1	2.2	2.4	1.8	2.0	1.3	1.4	1.9
Array 114H:	2.4	2.2	2.6	2.4	1.9	2.4	2.0	1.5	2.2

The array 107H was delivered to the Contract Monitor as a mechanical sample.

A single large 3 inch x 3 inch cell on H-Film had an efficiency of 1.6 percent at a maximum power point of 165 mA and 0.3 volts. Open circuit voltage and short circuit current were 0.45 V and 224 mA respectively.

Two other cells on H-Film were fabricated with evaporated metal electrodes on the n-type CdS instead of the usual soldered indium electrode. One cell had an evaporated nickel electrode and the other had an evaporated platinum electrode. In both cases, the electrode was very thin and was reinforced with air drying silver paint. The efficiencies were of the order of one percent which is probably attributable to film quality rather than the evaporated electrode. This point will be discussed further in another section.

3.2 Analysis of Slurry Samples

X-ray identification of copper slurry samples S-9 and S-21 indicates the

copper compound to be cuprous oxide, Cu_2O. There was no evidence of any other copper compound. The x-ray patterns were diffuse, probably due to lattice disorder and possibly due to particle size.

A qualitative, spectrographic, analysis of slurry samples S-18, S-21 and S-22 showed the following common components: copper, nickel, aluminum, magnesium and silicon. Samples S-21 and S-22 also showed iron. Rough estimates of quantities present indicate copper as the principal component for all samples. S-21 and S-22 contained nickel and silicon in the range 0.01 - 0.03 weight percent. All other constituents present were less than 0.03 weight percent. All the above elements except aluminum are reported as impurities in the lot analyses of the analytical reagents used in making the copper slurry. The source of aluminum contamination will be searched for and eliminated.

Electron micrographs were taken of the copper slurries. Slurry S-18, used extensively in making cells, had particle sizes in the range of 0.3 to 1.2 micron. The other slurry samples showed approximately the same range in particle size.

3.3 Metal Electrodes on n-Type CdS

In the First Quarterly Report[1] it was suggested that the indium peripheral electrode contacting the n-type CdS might be responsible for at least part of the deterioration observed. Indeed, this seemed to be borne out by the behavior of cell 102-7 which had an electroplated rhodium electrode in place of the indium. A number of metals were investigated as possible candidates for the role of contact to n-type CdS. Some were electroplated and some were vacuum evaporated. In a few instances, both methods were tried with the same metal. Successfully electroplated contacts were obtained with Ni, Rh, and Pt. Electroplated rhodium was quickly discarded because of its strongly acid plating bath. Any pinhole in the film was quickly attacked with subsequent lifting of the film around the hole. Rhodium would quickly plate out on both sides of the film. A similar result was observed at the edge of the film where lifting would occur rather often. Nickel,plated from a Watts type bath worked very well and this technique was employed on many of the cells made during this quarter. Platinum also gave good electrodes. One or two attempts to electroplate tin onto an electroplated nickel electrode quickly demonstrated that this was an undesirable material.

The resistance between two nickel stripes electroplated on a CdS film was compared with the resistance measured between two mercury-indium amalgam stripes of similar geometry. There was no significant difference between the two. An i-V plot obtained from one of the nickel stripes (compared with an amalgam stripe for reference) was a straight line through the origin even for quite high current densities of several amperes per square centimeter. Although nickel may be easily and quickly plated, it is considered undesirable to wet the CdS film with the plating solution.

Vacuum evaporated electrodes were considered next. Stripes of Ni, Al, Ag, Au, Cu, Mn, Mg, Cr, Sn, Pb, Fe, and Pt, were evaporated on CdS. In order to compare these various electrodes, a mercury-indium alloy stripe was placed on the CdS a short distance away from each. The i-V curve tracer using the 4-probe method was used to plot an i-V characteristic for current flowing into one contact, through the CdS film and out the other contact. Both voltage polarities were used. Whenever a straight line through the origin was obtained, the resistance of the contact-CdS combination was obtained from the slope of the i-V characteristic. This measurement was made for each electrode except platinum which was excluded simply because it was too difficult to evaporate a sufficiently thick layer.

The measurements were repeated after the film, with electrodes, had been heated on a 300°C hot plate in air. The data are summarized in Table 3-1.

These resistances are remarkably low. There is doubt about the validity of the last silver measurement because the silver stripe had been noticeably reduced in thickness and area and had turned quite black. For this same reason, manganese, magnesium, tin, lead and iron were eliminated. These metals are too easily oxidized and possibly sulfodized to be considered for reliable contacts. Thus, only gold, chromium, and nickel, are left after eliminating the non-ohmic contacts aluminum and copper. The principal objection to chromium and nickel is the difficulty of soldering to these metals. Gold on the other hand is inert, easily solderable and easy to evaporate. Therefore, several more evaporated gold stripes were evaporated on various CdS films and a careful examination of the Au-CdS contact was undertaken. Figure 3.1 shows the voltage current relationship for CdS film 147-2 between evaporated gold electrodes. These curves were obtained immediately after the gold evaporation. The gold electrodes are stripes one-inch long and 1/8-inch wide.

TABLE 3-1. Resistance Between Evaporated Metal Electrodes and In-Hg Amalgam Electrode. Heating was done on 300°C hot plate in air. i-V Characteristic Was Straight Line Through Origin Except Where Non-Ohmic Is Noted. Resistance Is Given In Ohms.

Heating Time Minutes	Al	Ag	Au	Cu	Mn	Mg	Cr	Ni	Sn	Pb	Fe
0	Non-ohmic	0.05	0.21	0.32	0.11	0.03	0.21	0.06	Non-ohmic	0.03	0.01
4	Non-ohmic	0.36	0.20	Non-ohmic					0.002	0.03	0.01
10	Non-ohmic	0.45	0.17	Non-ohmic	0.03	0.20	0.26	0.20	0.004	0.01	
20	Non-ohmic	0.11	0.16	Non-ohmic							

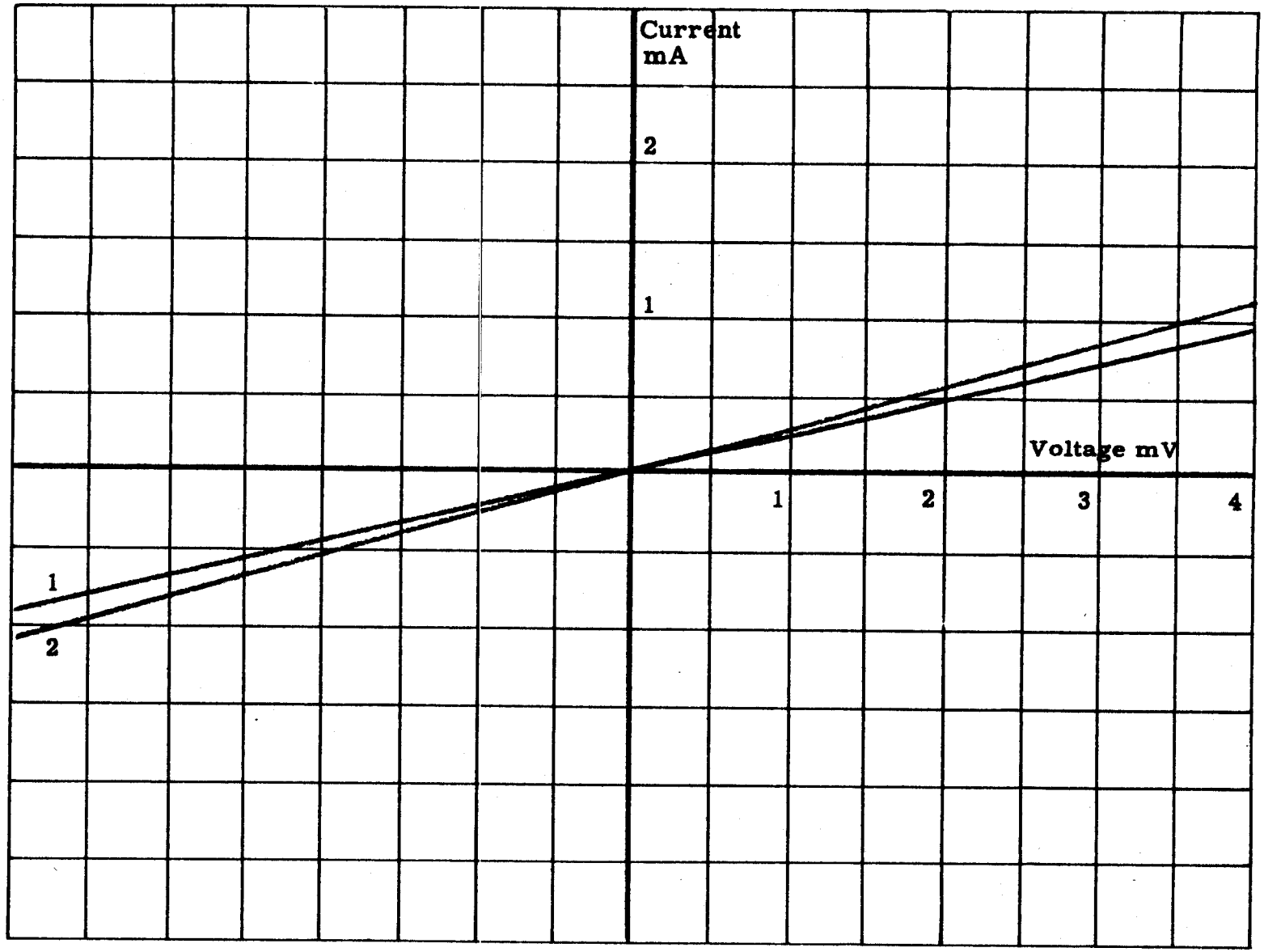

FIGURE 3. 1 VOLTAGE-CURRENT RELATIONSHIP FOR CdS FILM 147-2 BETWEEN EVAPORATED GOLD ELECTRODES. FOR CURVE 2, MULTIPLY SCALE BY 100.

The stripes were 11/16-inch apart In Fig. 3.1, curve 1 shows the linearity for a maximum current of 0.93 mA at 4 mV corresponding to a resistance of 4.3 ohm. The maximum current density was 1.15 mA-cm^{-2}, the area of the gold electrodes was 0.806 cm^{2}. Curve 2 shows the linearity for a maximum current of 112 mA at 400 mV, corresponding to a resistance of 3.58 ohms. The maximum current density in this case was 139 mA-cm^{-2}. The fact that the slopes of the curves are different show that gold electrodes are not truly ohmic. On the other hand, the fact that the slope changed only about 20 percent while the current density increased by a factor of more than 100 shows the departure from Ohm's law is quite small. It should be pointed out here that the resistivity of the cadmium sulfide film was 0.026 ohm-cm before heating.

After these measurements, the film was heated for one hour at 250°C in the oven used for processing photovoltaic cells. The measurements described above were repeated and the data are shown in Fig. 3.2. The heating decreased the resistance measured between the gold stripes. The slope of curve 1, Fig. 3.2 shows a resistance of 3.26 ohms for CdS 147-2 at 1.23 mA and 4 mV, and the slope of curve 2 shows a resistance of 2.76 ohms at 145 mA and 400 mV. The current densities are 1.53 mA-cm^{-2} and 180 mA-cm^{-2}, respectively.

Two indium-mercury amalgam stripes were painted on the films and the measurements repeated for current flowing between the two amalgam stripes, and between one gold and one amalgam stripe. Finally, an overlay of air dried silver paint was placed on each gold stripe and all the measurements repeated. Always, a straight line through the origin was obtained, and invariably, a small change in resistance accompanied a large change in current density. The data are summarized in Table 3-2. It is apparent that the resistance decreases when the current density increases and upon heating the films. The air drying silver paint applied to reduce the resistance of the gold film reduced the measured resistance and resistivity by more than half for CdS 147-2. The two gold stripes were 11/16-inch apart; the amalgam stripes were 5/16-inch apart. The resistivity, determined via the amalgam stripes was 4.1 x 10^{-3} ohm-cm. Therefore, the resistance of an 11/16-inch length of the CdS film should be 0.64 ohm. The resistance of this length of the film, measured via the gold electrodes was 1.27 ohms. Thus one may conclude that evaporated gold electrodes backed with silver paint, have about twice the contact resistance of amalgam electrodes. This does not mean, of course, that gold is the best electrode that one may put on n-type

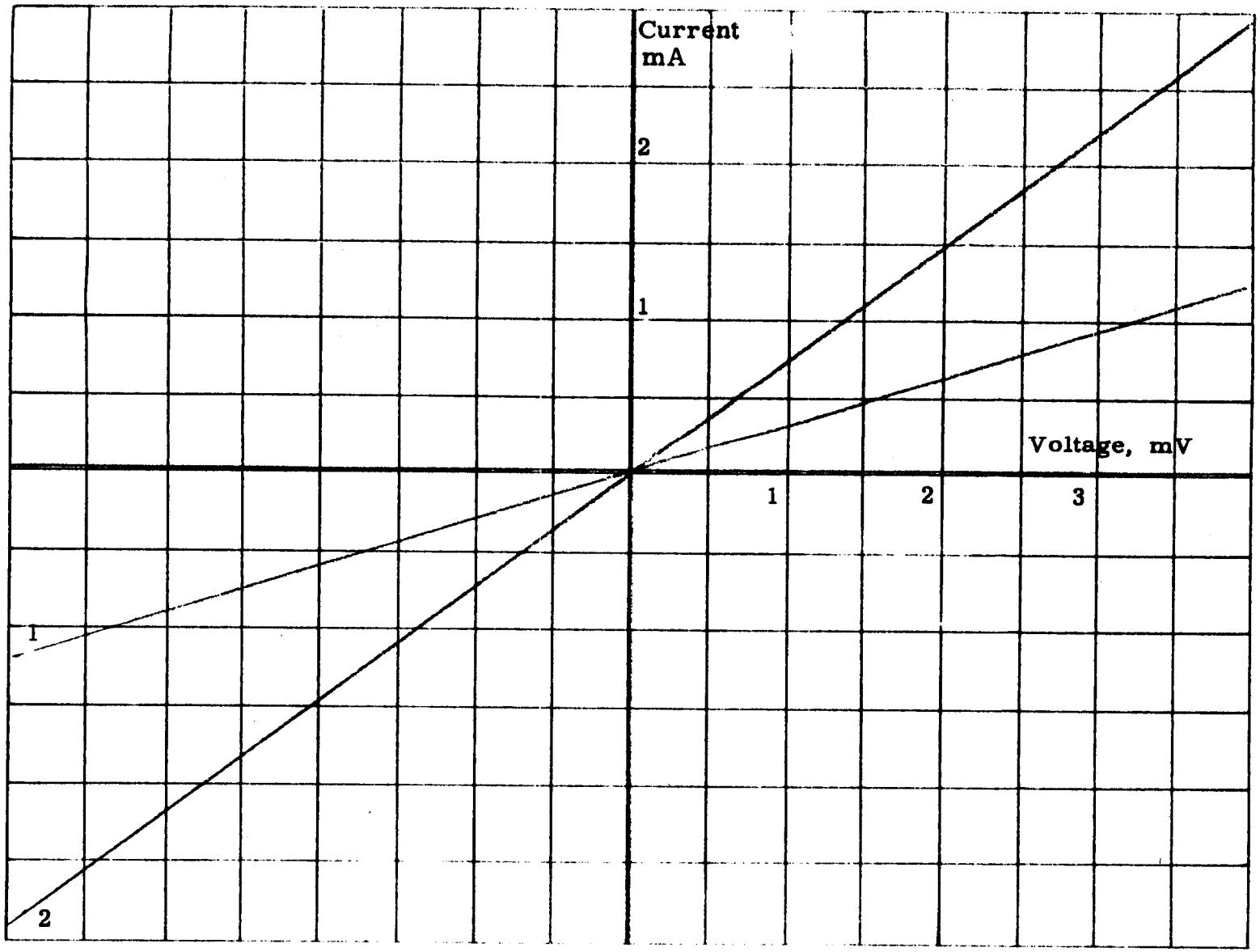

FIGURE 3. 2 MULTIPLY VERTICAL SCALE BY 100 AND HORIZONTAL SCALE BY 200 FOR CURVE 2.

TABLE 3-2. Resistance and Resistivity of CdS Film 147-2 Measured Between Evaporated Gold Electrodes and Mercury-Indium Amalgam Electrodes. Area of Electrodes was 0.806 cm^2.

	Current Density At Gold Electrode	Resistance Between Gold Electrodes	Current Density At Amalgam Electrode	Resistance Between Amalgam Electrodes	Resistivity of CdS Film Between Gold Electrodes	Resistivity of CdS Film Between Amalgam Electrodes
CdS 147-2						
Before Heating	1.15 mA-cm^{-2}	4.3 ohm				
	139 mA-cm^{-2}	3.6 ohm				
After Heating	1.53 mA-cm^{-2}	3.3 ohm	2.7 mA-cm^{-2}	0.93 ohm		
	180 mA-cm^{-2}	2.8 ohm	1.1 A-cm^{-2}	0.29 ohm	17.3 x 10^{-3} ohm-cm	4.1 x 10^{-3} ohm-cm
After Applying Silver Paint	0.8 A-cm^{-2}	1.2 ohm	1.1 A-cm^{-2}	0.29 ohm	8 x 10^{-3} ohm-cm	4.1 x 10^{-3} ohm-cm

CdS; but merely that it is the best convenient electrode. An obvious extension of this work is to examine electroplated gold electrodes in the same manner and also to look at the case where a gold overlay is placed on electroplated and evaporated nickel.

3.4 Optimizing Film Parameters

Whenever possible, film resistivity, carrier concentration and thickness are measured on at least one film sample from an evaporation. From the resistivity and carrier concentration the Hall mobility is calculated. These data have been analyzed and correlated with cell efficiency, open circuit voltage and short circuit current.

The result is a set of specifications such that a film, meeting these specifications, might reasonably be expected to yield good quality cells. These are:

Film Resistivity	0.025 ohm-cm - 0.035 ohm-cm
Carrier Concentration	8×10^{18} cm^{-3} - 10×10^{18} cm^{-3}
Hall Mobility	20 cm^2-$volt^{-1}$-sec^{-1} -27 cm^2-$volt^{-1}$-sec^{-1}
Thickness	50 microns - 60 microns

4. FILM CELL DETERIORATION

The phenomenon of cell deterioration has been discussed in a previous report and by others[2, 3]. In the First Quarterly Report[1], several significant instances were cited:

a) Unprotected cells deteriorated rapidly and completely.

b) Cells kept in a vacuum desiccator deteriorated completely but at a slower rate.

c) Cells from which indium was carefully eliminated deteriorated much more slowly. In time, they stabilized at an efficiency considerably lower than their initially measured efficiency.

d) In one instance, the efficiency of a cell with electroplated rhodium electrodes actually increased a little above its initial value and stabilized a value slightly higher than the initial value.

It was surmised from these observations that water vapor was the probable cause of the deterioration in a) above; that indium poisoning of the barrier was the probable

cause of the continued deterioration of the protected cells; and that impurities remaining on the barrier after processing was the probable cause of the behavior described in c) above.

There are other possible causes of deterioration, some of the more likely being: 1) an increase in series resistance, including contact and bulk resistance of the collector electrode; 2) leakage between electrodes due to moisture or similar causes; 3) changes in barrier properties due to temperature extremes or cycling; 4) imperfectly formed barriers containing areas of low resistance, or cracks or crazing leading to low resistance paths; and 5) diffusion of impurities along grain boundaries or precipitation of metallic phases along grain boundaries.

4.1 Characterization of Cell Deterioration

Whatever the cause of deterioration, the result is a decrease in cell efficiency manifested by decreases in one or more of the following: open circuit voltage, V_{oc}; short circuit current, i_{sc}; and the rectification ratio or fill factor, F. F.

The fill factor is defined as the maximum power output of the cell into a matched load divided by the product of the short circuit current and open circuit voltage. If V_m and i_m denote respectively the voltage and current at the maximum output power point, the efficiency of the cell is

$$\text{Cell Efficiency (\%)} = \frac{i_m \cdot V_m}{A\,E} \times 100$$

$$= \frac{F.F. \cdot V_{oc} \cdot i_{sc}}{A \cdot E} \times 100 \qquad (4\text{-}1)$$

where A is the effective area of the cell and E the incident radiant energy.

4.2 Modified Process

Long before any serious consideration had been given to deterioration and its causes, another problem had been noted: Whenever an evaporated metal electrode was deposited on the barrier layer, the resulting cell was low in efficiency and output voltage. It was reasoned that this was perhaps due to the evaporated metal finding its way into cracks or pores in the barrier and giving rise to low resistance

paths through the barrier layer. It was further reasoned that these paths might be eliminated by deeper diffusion and better lateral distribution of the diffused copper.

It was while looking into this problem that one solution to the deterioration problem was uncovered. It came about in the following manner: A cell had been coated with slurry and heated in the oven for 4 minutes at 250°C in the usual manner. It was air quenched and checked for photoactivity. It was photovoltaic. The slurry was removed by washing and brushing and dried for 5 minutes at 100°C in air. After cooling the photovoltaic effect had disappeared but photoconductivity was observed. The barrier was electroded with air drying silver paint and dried for 15 minutes. It was heated for 12 minutes at 250°C in the oven and air quenched. At this point, the photoconductivity had disappeared but the photovoltage had returned. An efficiency of about 0.5 percent was observed. Repeated heating in the oven for short times, followed by air quenching resulted in an increase in efficiency to a maximum of 1.3 percent. The change in efficiency with heating time is shown in the left side of Fig. 4.1. When additional heating failed to further increase the efficiency the cell was placed in the vacuum desiccator. At various 24-hour intervals the cell was removed long enough to measure its efficiency and immediately returned to the desiccator. The results for 12 days are shown in the right half of Fig. 4 1. This is the first instance in which rapid deterioration was not observed. The drop in efficiency after the 7th day is attributed to blistering of the silver electrode during processing. The peripheral electrode was electroplated nickel. After the 12th day the silver electrode was removed and replaced. The new electrode was allowed to dry tack-free at room temperature, then heated for 30 minutes at 100°C. Five minutes of heating at 250°C increased the short circuit voltage from 48 to 60 mA, but the open circuit voltage was reduced from 0.32 V to 0.21 V. Continued heating destroyed the cell.

No previous attempts had been made to obtain data relating cell parameters to photoactivation time largely because of the short (14 seconds to four minutes) photoactivation period. It was realized however that photoactivation must represent a period of build-up of cell parameters to an optimum value. What was not known was the manner in which the build-up occurred, i.e., the shape of the curve.

Other cells were made according to this modified process. The photoactivation curves and subsequent efficiencies are shown in Figs. 4.2 through 4.7. In each case, the final efficiency was at least as high as the highest achieved during

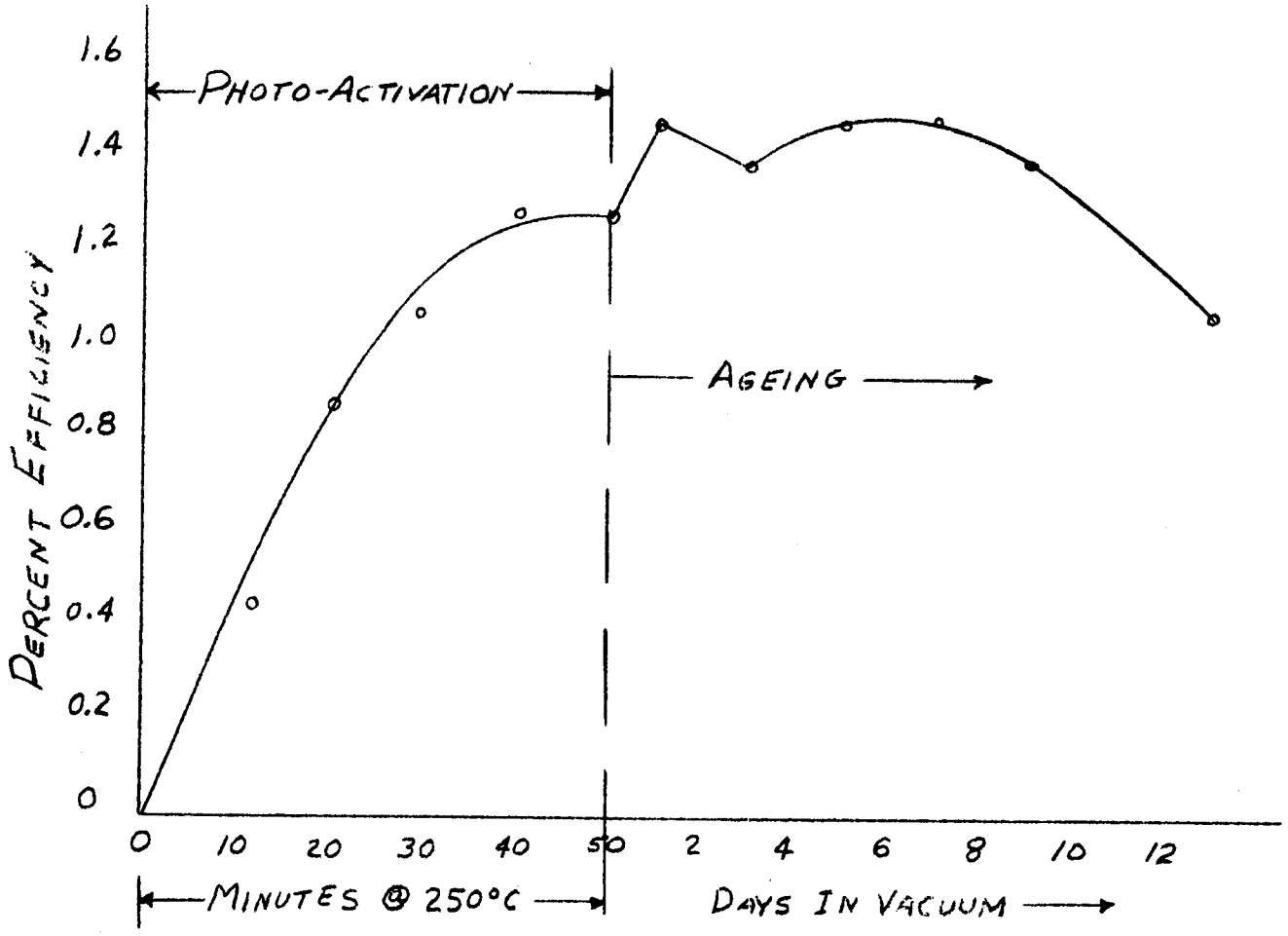

FIGURE 4.1 Showing the Ageing of a CdS Film Cell after Formation by the Modified Process.

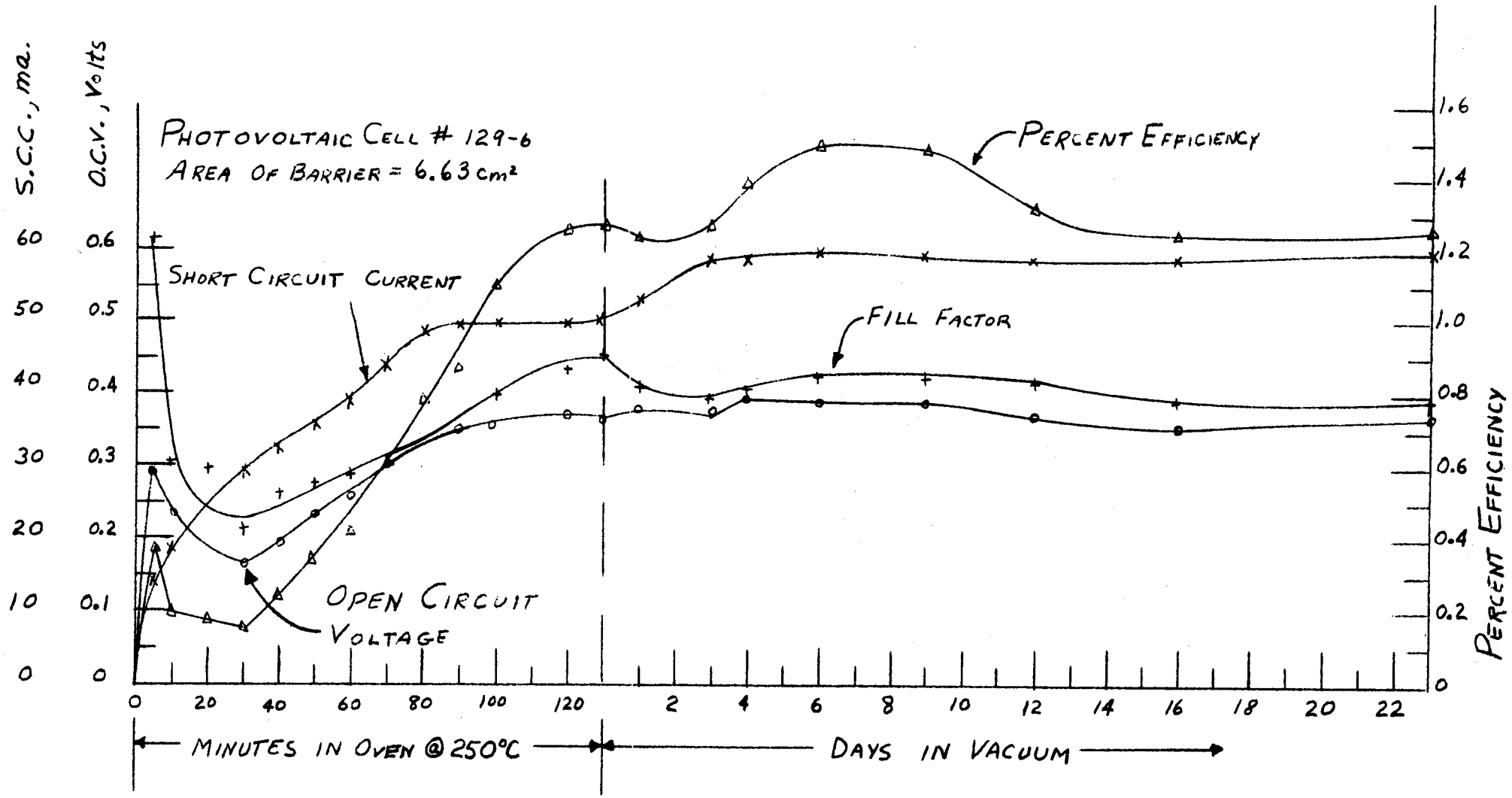

FIGURE 4-2. Photo-activation and Ageing of CdS Film Cell 129-6.

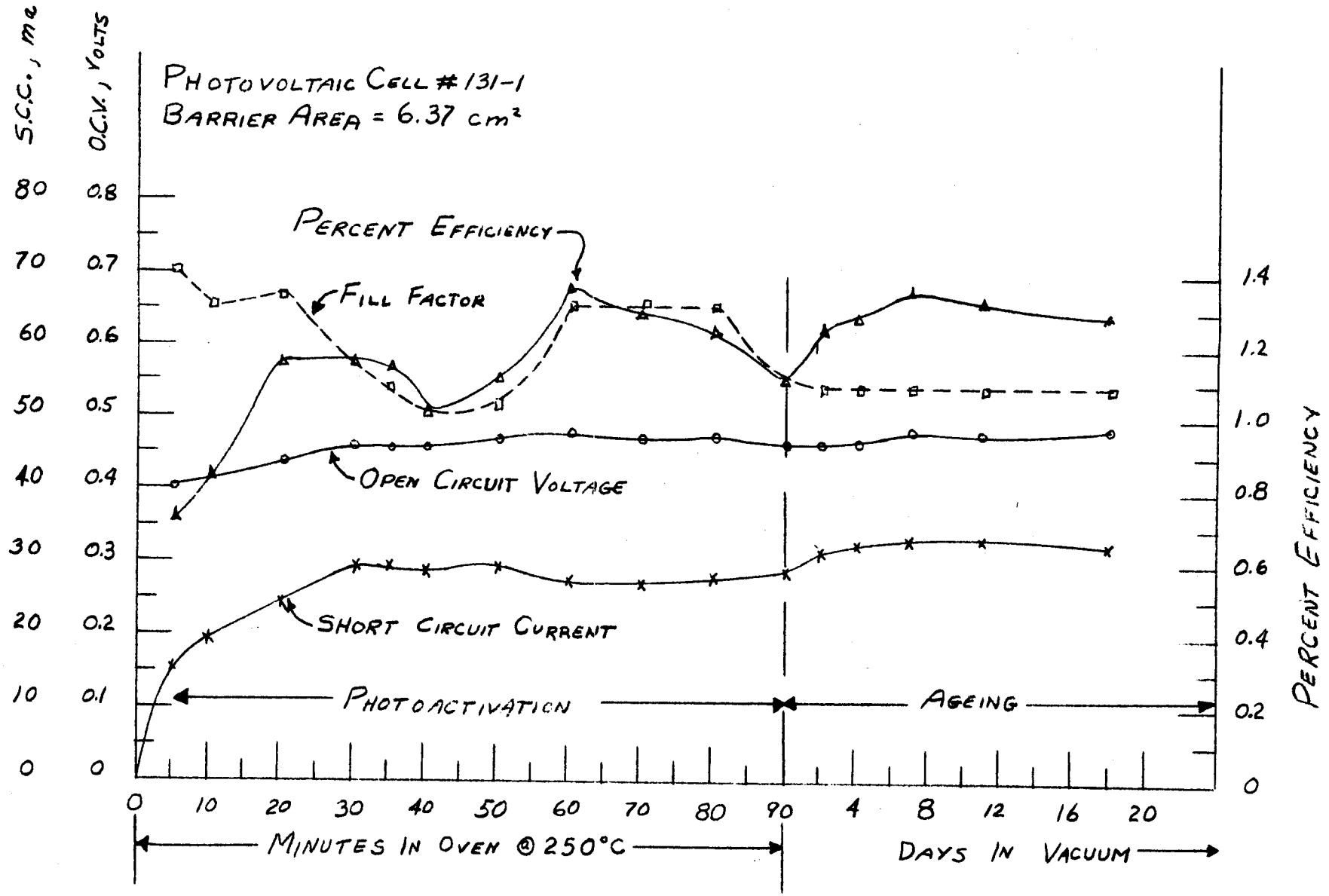

FIGURE 4.3 Photo-activation and Ageing of CdS Film Cell 131-1.

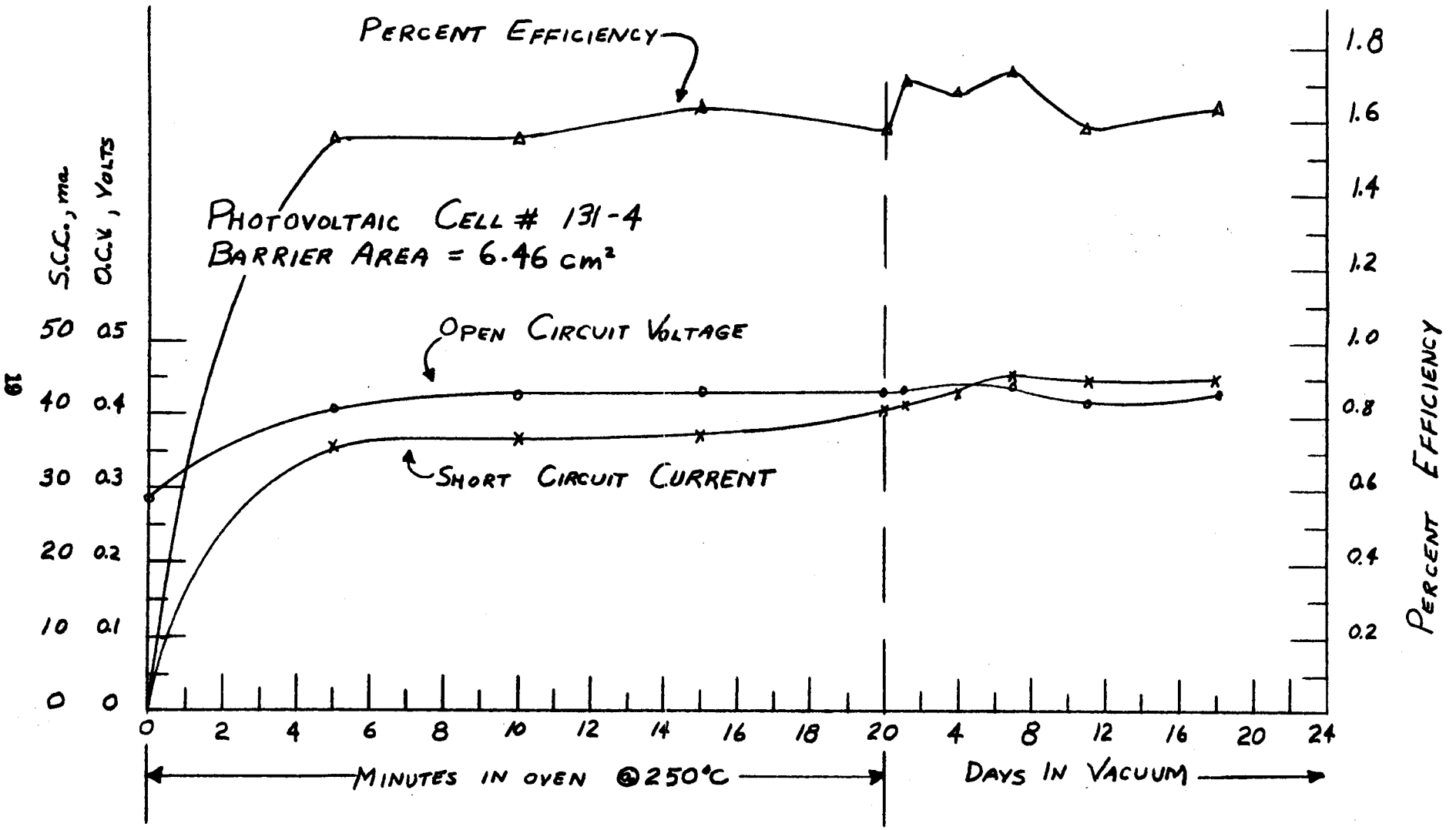

FIGURE 4.4 Photo-activation and Ageing of CdS Film Cell 131-4 Showing the Other Type of Activation Curve Observed.

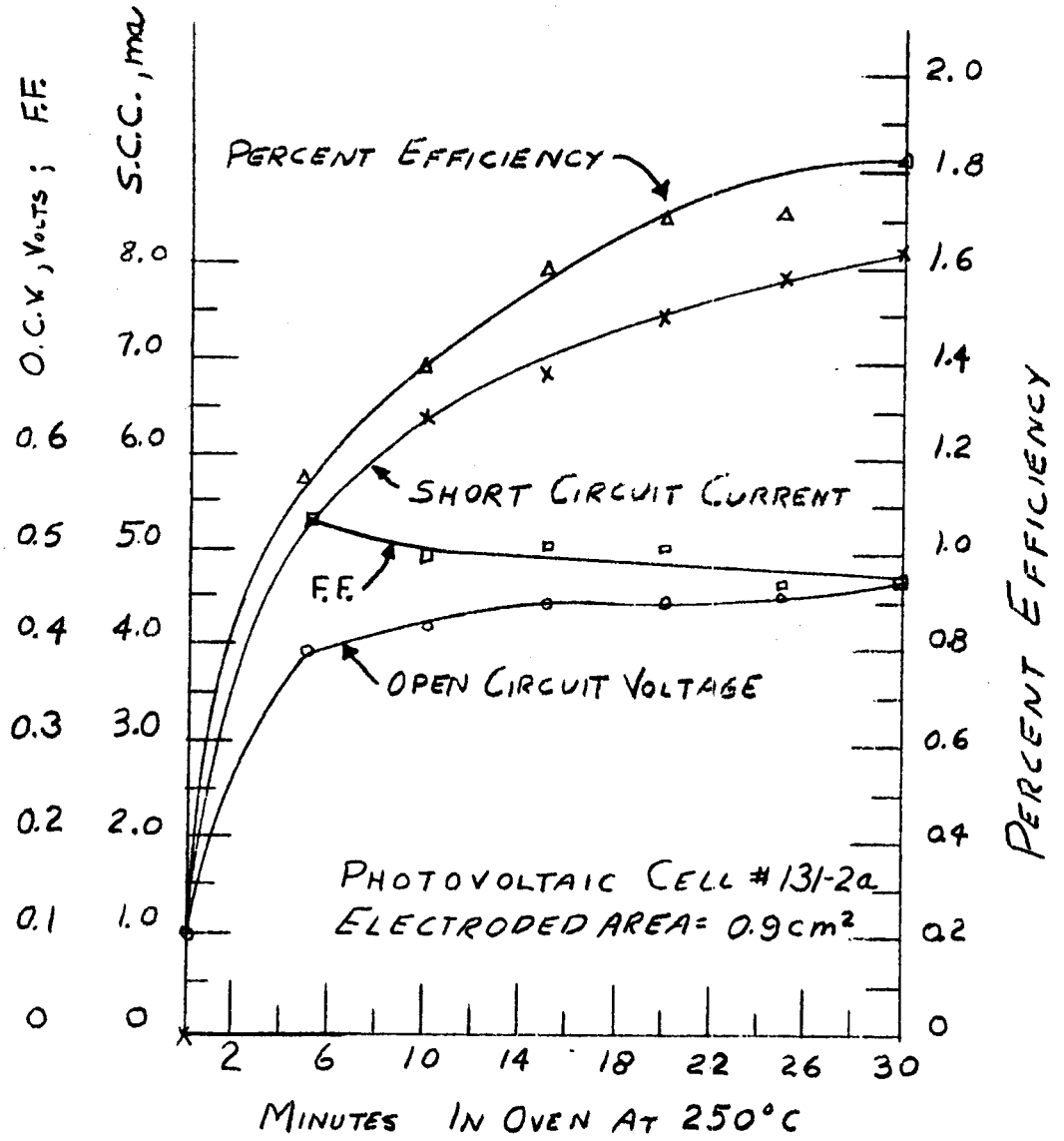

Figure 4.5 Photo-Activation Curve of CdS Film Cell 131-2a. This is a small area of Cell 131-2.

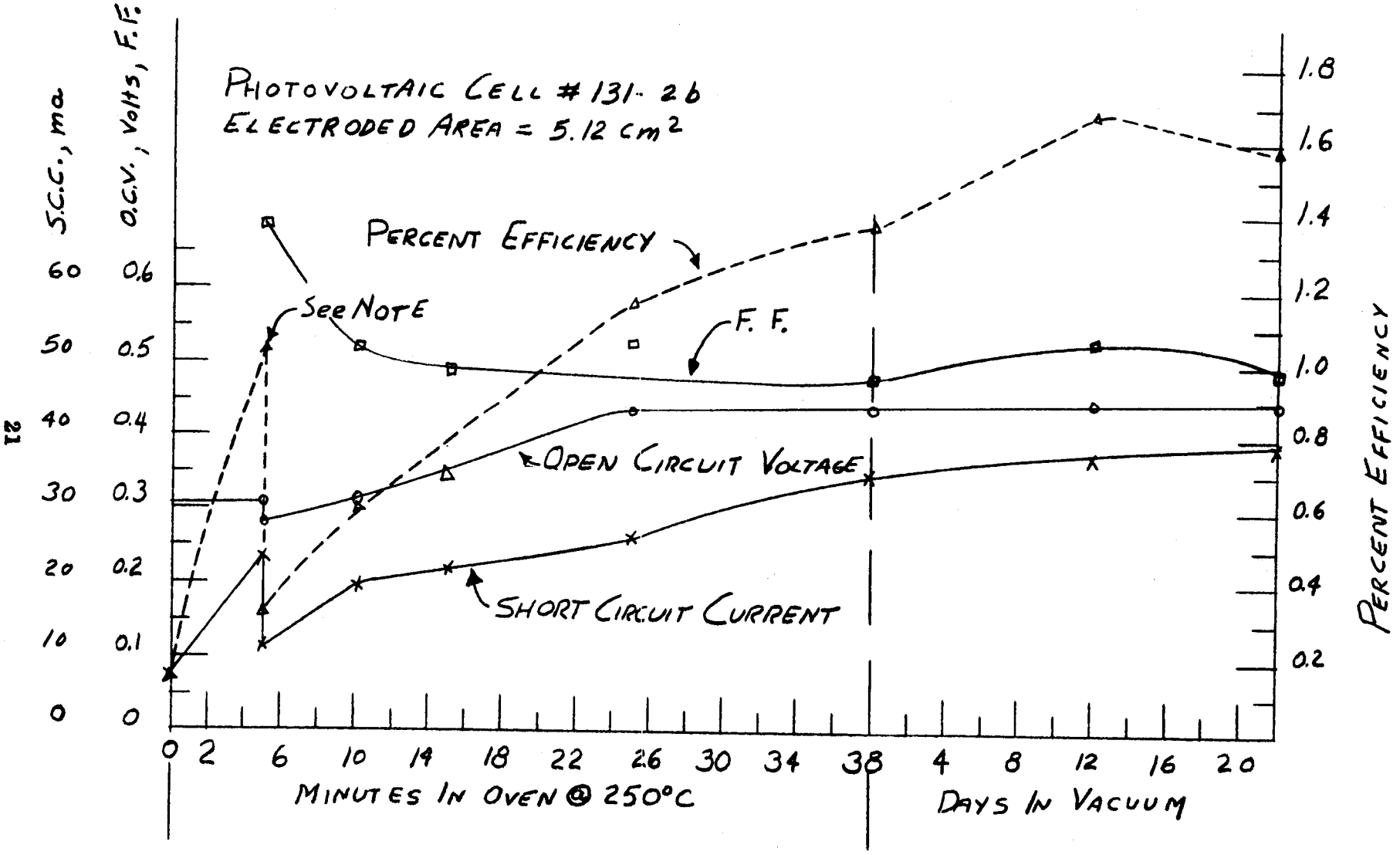

NOTE: Ag paste electrode blistered. Removed blisters & re-electroded

FIGURE 4.6 Photo-activation and Ageing Curve of CdS Film Cell 131-2b. This is a large area of Cell 131-2.

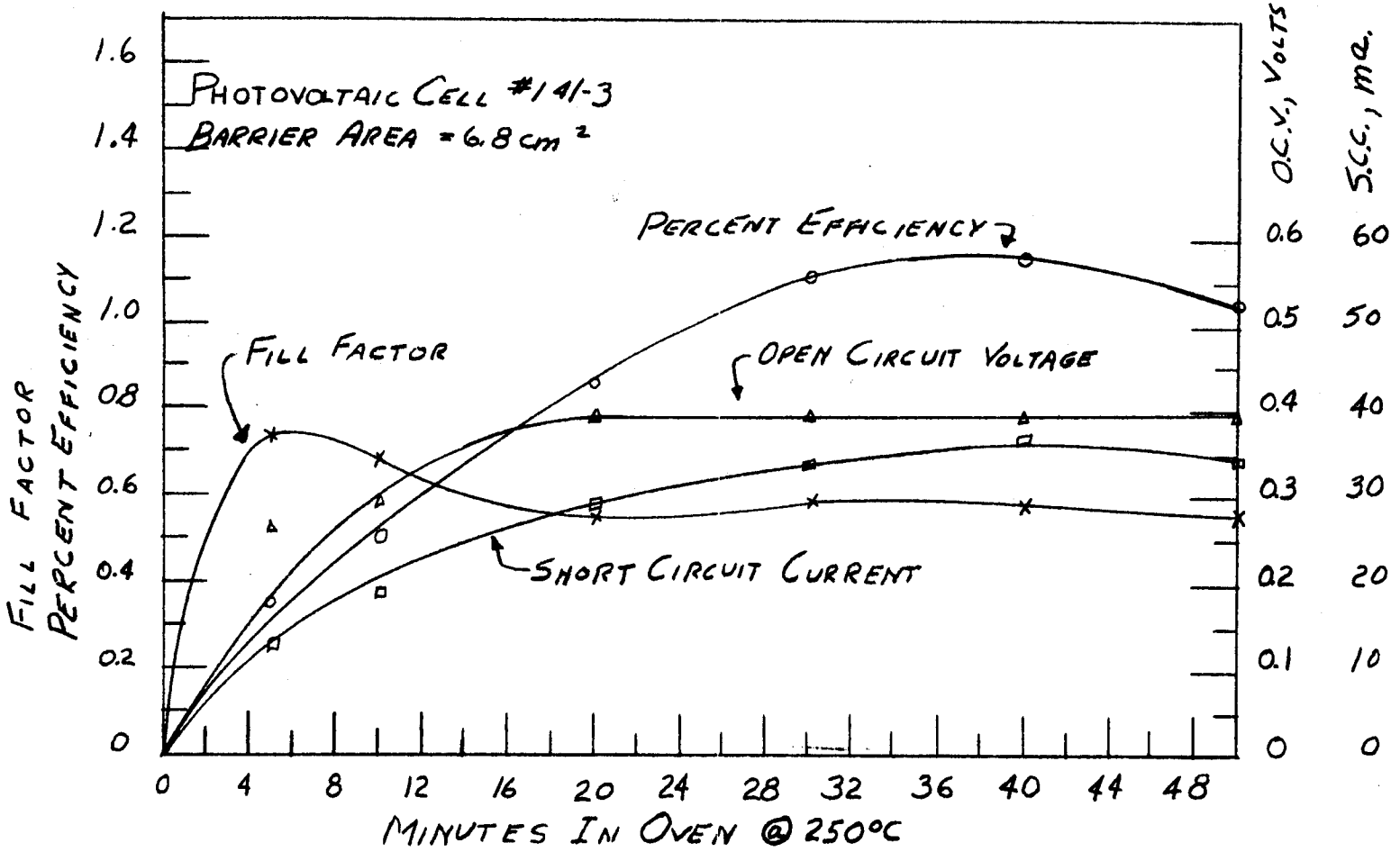

Figure 4.I Photo-Activation Curve of CdS Film Cell 141-3.

photoactivation. By way of contrast, Fig. 4.8 shows the behavior of a cell made according to the standard process. The final efficiency is considerably less than the initial efficiency.

It is recognized that the observed variations in the curves (Figs. 4.1 through 4.7) undoubtedly bear some relationship to more basic interval changes in the cell as well as to external variations in the electrodes, moisture, processing, etc. While these are not yet fully understood, it is expected that continued experimentation will eventually lead to a completely reproducible and reliable process for fabricating CdS photovoltaic cells.

4.3 Comparison between Standard and Modified Process

The differences between the standard process and the modified process become readily apparent through a step by step comparison.

STANDARD PROCESS	MODIFIED PROCESS
1. No step	1. Peripheral electrode applied. Electroplated or evaporated Ni, Au, etc., reinforced with Waldman's 3030 air drying silver paste.
2. Heat CdS film to 70-80°C.	2. Heat CdS film to 70-80°C.
3. Apply copper slurry to hot film.	3. Apply copper slurry to hot film. Allow slurry to dry.
4. Remove slurry; brushing and/or washing.	
5.a Heat film on 300°C hot plate for 14 seconds. Air quench.	4. Heat 4 minutes at 250°C in oven. Air quench.
5.b Heat film 4 minutes in 250°C oven.	
6. Apply peripheral electrode of indium. (This step has been replaced with a peripheral electrode of Ni or Au and may be done first).	6. Slurry removed: Brushing, washing.
7. Apply barrier electrode of Waldman's #3030 air dry silver paste.	7. Air dry film for 5 minutes at 80-100°C.
	8. Apply barrier electrode of Waldman's 3030 air dry silver paste. Dry tack free in 15 minutes. Heat additional 15 minutes at 175°C.
	9. Photoactivation process is begun by heating 5 to 10 minutes at a time in 250°C oven. Air quench between heatings. Continue until efficiency no longer increases.

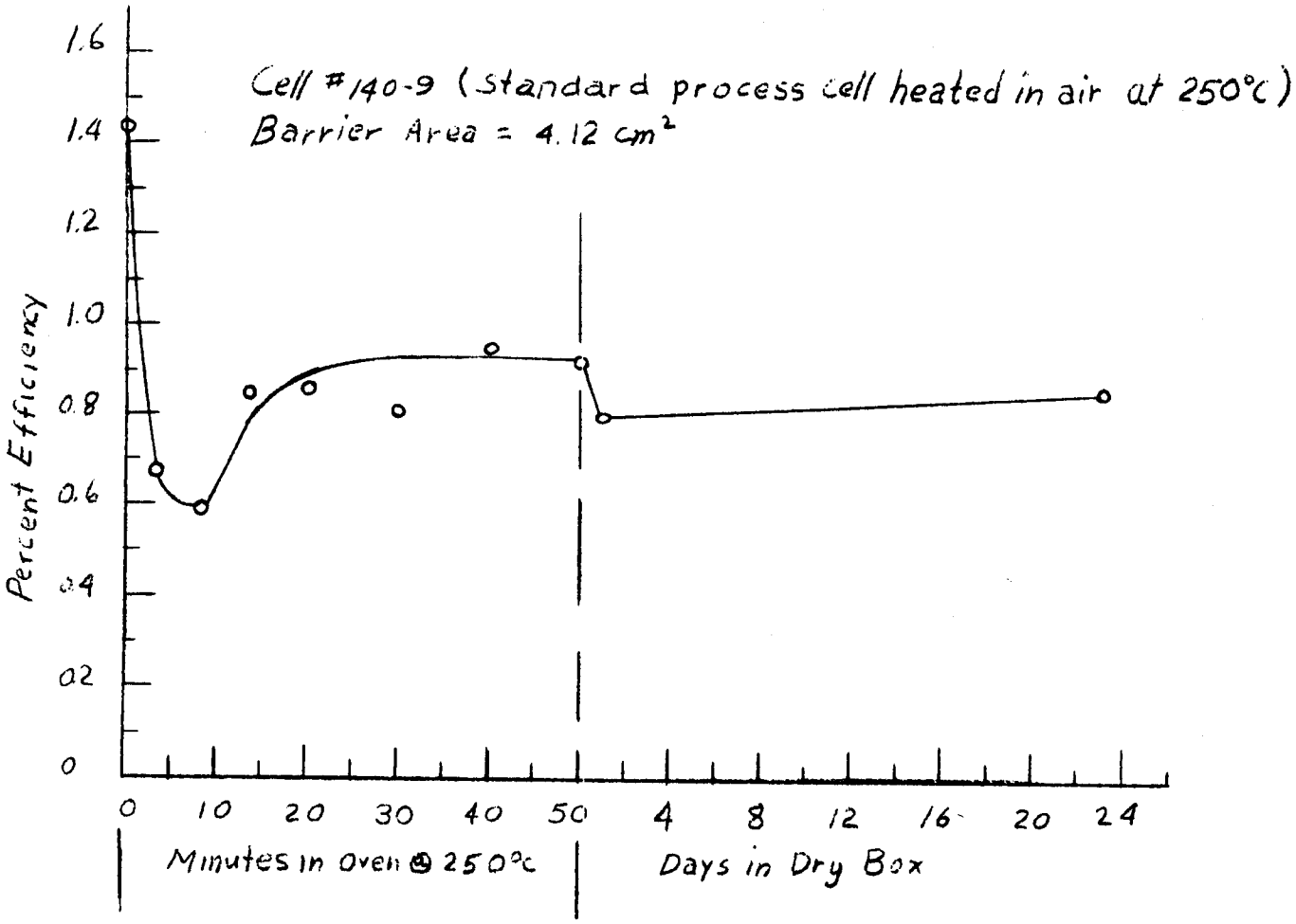

FIGURE 4.8 Photo-Activation and Ageing Curve of CdS Film Cell 140-9 Fabricated According to the Standard Process. Note that Initial Efficiency Is Much Higher Than Final Efficiency.

5. MATHEMATICAL MODELS

In the last quarterly report the subject of mathematical models for CdS photovoltaic cells was discussed in some detail and it was pointed out that none of the models suggested were very realistic. On the other hand, quite a lot of very useful information can be had from even a poor model. For this reason, the computer analysis described in the last report was carried out. The set of curves obtained were solutions of the equation

$$i = i_{\nu} - i_o(e^{\lambda(V-iR_s)}-1) + \frac{V - iR_s}{R_{sh}} , \qquad (5-1)$$

where i, V are respectively the current and voltage measured at the cell terminals, i_{ν} is the light generated current, i_o is the reverse saturation current, R_s and R_{sh} are the internal series and shunt resistances respectively and $\lambda = -q/AKT$ is a parameter involving the carrier change, q, the Boltzman constant, K, the absolute temperature, T, and a parameter, A, which is generally larger than 2, but is 1 for an ideal rectifier.

If R_s is very small, or equal to zero, and if R_{sh} is very large, a simpler equation is obtained:

$$i - i_{\nu} - i_o(e^{\lambda V}-1) . \qquad (5-2)$$

The computer analysis, while still incomplete, does indicate the following:

1) Increasing the series resistance, R_s, from zero rotates the forward characteristic clockwise about the point of intersection of the curve with the voltage axis, i.e. about the point representing open circuit voltage. This also has the effect of decreasing the fill factor. It does not affect the short circuit current point or the open circuit voltage, nor, in general, the shape of the curve for $V \leq \frac{1}{2}V_{oc}$ until R_s becomes quite large.

2) Decreasing the shunt resistance, R_{sh}, decreases the open circuit voltage point, but not the slope of the forward characteristic. The slope of the curve for $V \leq \frac{1}{2}V_{oc}$ depends almost entirely on the last term on the right of Eq. (5-1), but

except for appreciable values of R_s (i.e., $R_s > 0.1$ ohm for a 1 cm^2 cell) and very small values of R_{sh}, the short circuit current point is left unchanged. For $R_s >> 0.1$ ohm, the short circuit current decreases. The fill factor is also reduced when R_{sh} becomes small.

3) If the parameter, A, is increased from 1 to 3, the fill factor is significantly reduced for all values of R_s and R_{sh}. The slope of the forward characteristic is decreased just as occurs for higher series resistance. The slope of the curve for $V < \frac{1}{2}V_{oc}$ is relatively unaffected by changes in A.

4) It is difficult to distinguish between the effects of A and R_s on the forward characteristic.

It is expected that other generalizations and insights will become apparent as the computer analysis is continued.

5.1 The Simple Model

Equation (5-1) is extremely difficult to handle because of its being transcendental in three of the parameters. Equation (5-2) is much easier to manipulate and interesting results obtain when various simple manipulations are carried out.

5.1.1 The Maximum Power Point

The simple graphical determination of the maximum power point is derived by differentiating the expression for electrical power:

$$P = iV. \tag{5-3}$$

Differentiating with respect to V, and setting $\frac{dP}{dV} = 0$ to obtain the maximum point of the curve, one obtains

$$\frac{di}{dV} = \frac{-i_m}{V_m}, \tag{5-4}$$

which states that the slope of the tangent line at the maximum power point is equal to the ratio of the coordinates of the maximum power point. Simple geometry shows that if one draws the tangent line to the maximum power point of a typical i-V characteristic curve, then the maximum power point bisects the tangent line between its

intercepts with the axes. This gives a rapid, simple and accurate determination of the maximum power point on any experimental i-V curve.

If, now, one applies this approach to Eq. (5-2), one obtains a rather elegant determination of V_m or λ.

Multiply both sides of Eq. (5-2) by V and obtain

$$P = iV = i_\nu V - i_o(e^{\lambda V}-1)V. \tag{5-5}$$

Differentiate both sides with respect to V and obtain

$$\frac{dP}{dV} = i_\nu + i_o - i_o e^{\lambda V}(1 + \lambda V). \tag{5-6}$$

At the maximum power point, $V = V_m$, $i = i_m$, and $\frac{dP}{dV} = 0$, therefore

$$\frac{i_\nu + i_o}{i_o} = e^{\lambda V_m}(1 + \lambda V_m). \tag{5-7}$$

It is possible to express i_ν and i_o in terms of V_{oc}, for, from Eq. (5-2) when $V = V_{oc}$, $i = 0$, and

$$\frac{i_\nu + i_o}{i_o} = e^{\lambda V_{oc}}. \tag{5-8}$$

Therefore, combining Eqs. (5-7) and (5-8),

$$e^{\lambda V_{oc}} = e^{\lambda V_m}(1 + \lambda V_m). \tag{5-9}$$

Thus, if λ is known, V_m may be obtained and if V_m is known, λ may be obtained. CdS cell 65-6A had an efficiency of 3.4 percent, $V_{oc} = 0.5$ volt and $V_m = 0.38$ volt According to Eq. (5-9)

$$\lambda = 16.6. \tag{5-10}$$

For room temperature, $T = 293°K$; and $K = 1.38 \times 10^{-23}$ joule - $°K^{-1}$ and $q = -1.6 \times 10^{-19}$ coulomb. Then, since $\lambda = \frac{-q}{AKT}$,

$$A = 2.39. \tag{5-11}$$

It is possible to obtain values of A graphically from semi-log plots of i-V characteristics. Ideally, these would be straight lines whose slopes are numerically equal to λ. In practice, however, the semi-log plots are not straight lines except for the higher efficiency cells. One such cell was CdS 49-8 which had an efficiency of 2.14 percent and when plotted semi-logarithmically yielded two values of λ corresponding to $A = 3.44$ and $A = 4.16$. The maximum power point coordinates were $i_m = 23.5$ mA, $V_m = 0.29$ volt and V_{oc} was 0.43 volt. By Eq. (5-9), $\lambda = 9.4$ corresponding to $A = 4.2$ in good agreement with the larger of the two graphically obtained values. For a very poor cell, CdS 37-2, which had an efficiency of only 0.38 percent, the graphically determined A was 6.4. The maximum power point coordinates were $i_m = 25$ mA, $V_m = 0.105$ volt, and $V_{oc} = 0.19$ volt. Equation (5-9) gives for λ, the value 5.0 corresponding to $A = 7.75$ which is not in very good agreement with the graphically determined A. This is to be expected, however, because the poorer cells usually have series and shunt resistances which cannot be ignored as was done in deriving Eq. (5-9).

5.1.2 Ratio of i_ν/i_o

From Eq. (5-8) one may calculate the ratio of i_ν/i_o in terms of V_{oc}. It is

$$\frac{i_\nu}{i_o} = e^{\lambda V_{oc}} - 1. \tag{5-12}$$

In principle, this ratio can be determined from the light and dark i-V characteristics, but generally, the reverse saturation current is too small to measure accurately. Furthermore, since the i-V characteristics do have significantly large slopes in the reverse bias condition, the experimental cells do not agree well enough with the ideal model of Eq. (5-2) to warrant the extra labor of the measurement. However, it is instructive to calculate the ratios for the three cases cited in

Section 5.11. It is convenient to use current densities for this calculation because of the variations in cell areas. For cell 65-6A, which had $V_{oc} = 0.50$ volt and $\lambda = 16.6$,

$$\frac{i_\nu}{i_o} = e^{16.6 \times 0.50} - 1 = 4.02 \times 10^3. \qquad (5\text{-}13)$$

The short circuit current density of this cell was 12.4 mA-cm^{-2}, and this must be very nearly the value of i_ν, therefore, $i_o = 3.1 \times 10^{-6}$ amp-cm^{-2}.

For cell 49-8 with $j_{sc} = 12.1$ mA-cm^{-2}, $V_{oc} = 0.43$ volt and $\lambda = 9.4$,

$$\frac{i_\nu}{i_o} = e^{9.4 \times 0.43} - 1 = 55.8, \qquad (5\text{-}14)$$

and $i_o = 0.22 \times 10^{-3}$ amp-cm^{-2}.

And finally, for cell 37-2, $j_{sc} = 6.97$ mA-cm^{-2}, $V_{oc} = 0.19$ volt and $\lambda = 5.0$,

$$\frac{i_\nu}{i_o} = e^{5.0 \times 0.19} - 1 = e^{0.95} - 1 = 1.59. \qquad (5\text{-}15)$$

and

$$i_o = 4.4 \times 10^{-3} \text{ amp-cm}^{-2}.$$

6. ALTERNATE METHODS OF PRODUCING FILMS

This work was terminated at the end of February, 1964. Although excellent chemically deposited CdS mirrors were made, it was not possible to obtain resistivities low enough to form good backwall CdS photovoltaic cells. The work done in this quarter is summarized below.

It has already been reported that the thickness of CdS films on pyrex plates could be built up from a few hundred angstroms to a few microns by repeating

the process of deposition a number of times. X-ray diffraction patterns were fuzzy, revealing very small grain size. The only strong lines present indicated an intermediate structure between the cubic and the hexagonal. The c-axes were mainly perpendicular to the surface. The resistance of these films was very high, of the order of 10^{10} - 10^{12} ohm. The hope that heat treatment would produce films composed of large grains with organized structure (hexagonal only) and also having substantially lower resistance was not realized.

One film heated to 600°C in vacuum completely evaporated from the substrate in 45 minutes. Microscopic examination of another film which was held at 500°C in argon for 45 minutes showed extensive formation of blisters, and separation of the deposited layers from each other. A third film was wetted with concentrated $CdCl_2$ solution, dried, then heated to 560°C in argon. The $CdCl_2$ was to act as a flux, aiding recrystallization and grain growth. This film developed a network of fine cracks. The particles were about .03 mm across, hexagonal by x-ray, and having their c-axes mainly parallel to the substrate.

Other investigations were carried out using test tubes containing the pyrex plates (5 x 2 x 0.2 cm) which, after thorough cleaning, were preseeded by immersion for 1/2 hour in a freshly prepared colloidal suspension of CdS. Two sets of experiments were carried out. One set with mixtures of equal volumes of the solutions of $CdC1_2$, thiourea and NH_2OH. In the other set thiosinamine was used instead of thiourea. It was observed that the higher the NH_4OH concentration, the longer the time required for the solution to become cloudy and begin film formation. With thiourea and 3N NH_4OH clouding took about 3 minutes, but with 6N NH_4OH about 30 minutes were required. The corresponding times for thiosinamine were approx. 9 and 90 minutes. After the initial CdS film formation and clearing of the supernatant liquid the test tubes were placed into a water bath at 65°C for 1 hour. During this period more CdS precipitated out. Finally the solutions were boiled for 1/2 hour.

All films were well adhering and glossy. Film thicknesses were computed from weight increment and surface area of the pyrex plates and CdS density (4.82 g/cm^3).

It is appropriate at this time to speculate on the mechanism of the film formation. It seems to be essential that the reaction resulting in CdS should proceed slowly. It is possible that the Cd and S ions combine on the pyrex surface and become attached to it. It is also conceivable that nearby colloidal CdS particles diffuse to the surface which attacks them. One would expect slow reactions to occur in intermediate steps. This is the case with the complex Cd compound:

$$\left[Cd(NH_3)_4\right]^{++} \rightleftharpoons \left[Cd(NH_3)_3\right]^{++} + NH_3 , \tag{6-1}$$

$$\left[Cd(NH_3)_3\right]^{++} \rightleftharpoons \left[Cd(NH_3)_2\right]^{++} + NH_3 , \tag{6-2}$$

$$\left[Cd(NH_3)_2\right]^{++} \rightleftharpoons \left[Cd(NH_3)\right]^{++} + NH_3 , \tag{6-3}$$

$$\left[Cd(NH_3)\right]^{++} \rightleftharpoons \left[Cd^{++} + NH_3\right] . \tag{6-4}$$

All these species are present in the solution, and their respective concentrations are governed by the mass action law:

$$k_1 = \frac{\left[Cd(NH_3)_3\right]^{++} \cdot \left[NH_3\right]}{\left[Cd(NH_3)_4\right]^{++}} , \tag{6-5}$$

$$k_2 = \frac{\left[Cd(NH_3)_2\right]^{++} \cdot \left[NH_3\right]}{\left[Cd(NH_3)_3\right]^{++}} ; \text{ and} \tag{6-6}$$

similarly for k_3 and k_4. These equilibrium constants are also called "instability constants."

The summary equilibrium reaction is

$$\left[Cd(NH_3)_4\right]^{++} \rightleftharpoons Cd^{++} + 4NH_3 , \tag{6-7}$$

with

$$K = \frac{[Cd]^{++} \cdot [NH_3]^4}{[Cd(NH_3)_4]^{++}} \quad . \tag{6-8}$$

K is the "overall" instability constant. The Literature generally gives log 1/K = pK. For this particular case[4] ($K = 7.56 \times 10^{-8}$), and

$$pK = 7.12. \tag{6-9}$$

As can be seen, an excess of NH_3 in the solution will strongly reduce the concentration of the Cd ions since this is inversely proportional to the 4th power of the NH_3 concentration. In fact, if the concentration of NH_3 is very high (close to 15N), practically no CdS will form because the Cd^{++} concentration will be lowered to about 10^{-14} moles/liter and this value is too close to that of the Cd concentration expressed in the solubility product of CdS ($K_{sp} = 316 \times 10^{-29}$).

The release of S^{--} from thiosinamine presumably takes place in three steps:

$$CH_2 = CH \cdot CH_2 \cdot NH \cdot CS \cdot NH_2 \rightleftharpoons CH_2 = CH \cdot NH \cdot CN + H_2S, \tag{6-10}$$

$$H_2S \rightleftharpoons H^+ + HS^-,$$

$$HS^- \rightleftharpoons H^+ + S^{--}.$$

Because the degree of dissociation of thiosinamine in aqueous solution is very small, the concentration of S^{--} will also be very low.

The ionic reaction

$$Cd^{++} + S^{--} \longrightarrow \underset{\downarrow}{CdS}, \tag{6-11}$$

is practically instantaneous, but the reaction (summary)

$$Cd(NH_3)_4^{++} + CH_2 = CH \cdot CH_2 \cdot NH \cdot CS \cdot NH_2 \longrightarrow$$

$$CH_2 = CH \cdot CH_2 \cdot NH \cdot CN + \underset{\downarrow}{CdS} + 4NH_3 + 2H^+, \qquad (6\text{-}12)$$

is a relatively slow rate process. The reason is that in the same measure as minute amounts of Cd^{++} and S^{--} combine to CdS the equilibrium concentrations of all aforementioned species is upset. They require constant adjustment according to the mass action law until the CdS precipitation is completed.

7. CORRIGENDA

Errors in the First Quarterly Report have been pointed out. On page 15, Eq. (4-3), instead of 0.0102 read 0.102; and on the following line, instead of "Thus only 1.02 percent . . ." read "Thus only 10.2 percent". . . ;
and finally, on the next to the last line of the section, instead of "97 percent . . ." read ". . 88 percent . . " .

8. WORK PLANNED FOR NEXT QUARTER

In the next quarter, emphasis will be placed on transferring to H-Film substrates the type of films that have been produced on glass substrates; films, with efficiencies in the 2 to 2.5 percent range, which do not deteriorate when protected from moisture and the laboratory ambient. The H-Film curling problem will be studied intensely. Experiments based on pre-stressing the H-Film are planned as well as experiments on modifying the embossing die.

Continued attention will be given the problems of electroding, of barrier formation and mathematical analysis.

9. ACKNOWLEDGEMENT

The assistance of Mary Ellen Rander, who programmed and operated Clevite's Burroughs B-5000 Digital Computer, is gratefully acknowledged.

10. REFERENCES

1. W.J. Deshotels, et al., "Study of Thin Film Large Area Photovoltaic Solar Energy Converter," First Quarterly Report, January 23, 1964, Contract No. NAS 3-2795 pp. 11-13.

2. F.A. Shirland, et al., "Research on Solar Energy Conversion Employing Cadmium Sulfide," ASD Technical Report 62-69, Vol. I, January, 1962, pp. 34-39; Vol. II, December, 1962, pp. 40-45.

3. R.R. Chamberlin and J.S. Skarman, "Feasibility Investigation of Chemically Sprayed Thin Film Photovoltaic Converters," Fourth Quarterly Report, Contract No. AF 33(657)-7919, 1 February 1963 through 30 April, 1963, pp. 11-13.

4. K.B. Yatsimirskii and V.P. Vasil'er, "Instability Constants of Compounds," (Pergamon Press, New York, 1960), p. 94.